REPORT DOCUMENTATION PAGE

FORM APPROVED
OMB No. 0704-0188

1. AGENCY USE ONLY (Leave blank)	2. REPORT DATE	3. REPORT TYPE AND DATES COVERED
	June 14, 1995	Interim Quarterly Progress Report for March 1, 1995 through May 31, 1995

4. TITLE AND SUBTITLE OF REPORT
Quarterly Progress Report on Visible Light Emitting Materials and Injection Devices.

5. FUNDING NUMBERS
G:N-00014-92-J-1895

6. AUTHOR(S)
Paul H. Holloway

7. PERFORMING ORGANIZATION NAME(S) AND ADDRESS(ES)
University of Florida
Dept. of Materials Science and Engineering
P.O. Box 116400
Gainesville, FL 32611-6400

8. PERFORMING ORGANIZATION REPORT NUMBER:
N/A

9. SPONSORING/MONITORING AGENCY NAME(S) AND ADDRESS(ES)
Office of Naval Research
Dr. Y.-S. Park
Electronics/Electro-Optics -- Code: 1212
Department of the Navy
Arlington, VA 22217-5000

10. SPONSORING/MONITORING AGENCY REPORT NUMBER:

11. SUPPLEMENTARY NOTES:

12a. DISTRIBUTION AVAILABILITY STATEMENT
Unlimited

12b. DISTRIBUTION CODE

13. ABSTRACT (Maximum 200 words)

A report is given on progress of our research into ZnSe-based GaN-based materials and devices for light emitting diodes and diode lasers.

14. SUBJECT TERMS
Zinc Selenide
Gallium Nitride
Light Emitting Diodes
Diode Lasers

15. NUMBER OF PAGES:
19 + cover

16. PRICE CODE

17. SECURITY CLASSIFICATION OF REPORT:	18. SECURITY CLASSIFICATION OF THIS PAGE	19. SECURITY CLASSIFICATION OF ABSTRACT	20. LIMITATION OF ABSTRACT
Unclassified	Unclassified	Unclassified	Unlimited

GENERAL INSTRUCTIONS FOR COMPLETING SF 298

The Report Documentation Page (RDP) is used in announcing and cataloging reports. It is important that this information be consistent with the rest of the report, particularly the cover and title page. Instructions for filling in each block of the form follow. It is important to ***stay within the lines*** to meet ***optical scanning requirements.***

Block 1. Agency Use Only *(Leave blank)*.

Block 2. Report Date. Full publication date including day, month, and year, if available (e.g. 1 Jan 88). Must cite at least the year.

Block 3. Type of Report and Dates Covered. State whether report is interim, final, etc. If applicable, enter inclusive report dates (e.g. 10 Jun 87 - 30 Jun 88).

Block 4. Title and Subtitle. A title is taken from the part of the report that provides the most meaningful and complete information. When a report is prepared in more than one volume, repeat the primary title, add volume number, and include subtitle for the specific volume. On classified documents enter the title classification in parentheses.

Block 5. Funding Numbers. To include contract and grant numbers; may include program element number(s), project number(s), task number(s), and work unit number(s). Use the following labels:

C	- Contract	PR	- Project
G	- Grant	TA	- Task
PE	- Program Element	WU	- Work Unit Accession No.

Block 6. Author(s). Name(s) of person(s) responsible for writing the report, performing the research, or credited with the content of the report. If editor or compiler, this should follow the name(s).

Block 7. Performing Organization Name(s) and Address(es). Self-explanatory.

Block 8. Performing Organization Report Number. Enter the unique alphanumeric report number(s) assigned by the organization performing the report.

Block 9. Sponsoring/Monitoring Agency Name(s) and Address(es). Self-explanatory.

Block 10. Sponsoring/Monitoring Agency Report Number. *(If known)*

Block 11. Supplementary Notes. Enter information not included elsewhere such as: Prepared in cooperation with...; Trans. of...; To be published in.... When a report is revised, include a statement whether the new report supersedes or supplements the older report.

Block 12a. Distribution/Availability Statement. Denotes public availability or limitations. Cite any availability to the public. Enter additional limitations or special markings in all capitals (e.g. NOFORN, REL, ITAR).

DOD	- See DoDD 5230.24, "Distribution Statements on Technical Documents."
DOE	- See authorities.
NASA	- See Handbook NHB 2200.2.
NTIS	- Leave blank.

Block 12b. Distribution Code.

DOD	- Leave blank.
DOE	- Enter DOE distribution categories from the Standard Distribution for Unclassified Scientific and Technical Reports.
NASA	- Leave blank.
NTIS	- Leave blank.

Block 13. Abstract. Include a brief *(Maximum 200 words)* factual summary of the most significant information contained in the report.

Block 14. Subject Terms. Keywords or phrases identifying major subjects in the report.

Block 15. Number of Pages. Enter the total number of pages.

Block 16. Price Code. Enter appropriate price code *(NTIS only)*.

Blocks 17. - 19. Security Classifications. Self-explanatory. Enter U.S. Security Classification in accordance with U.S. Security Regulations (i.e., UNCLASSIFIED). If form contains classified information, stamp classification on the top and bottom of the page.

Block 20. Limitation of Abstract. This block must be completed to assign a limitation to the abstract. Enter either UL (unlimited) or SAR (same as report). An entry in this block is necessary if the abstract is to be limited. If blank, the abstract is assumed to be unlimited.

Quarterly Progress Report

March 1, 1995 to May 31, 1995

Visible Light Emitting Materials and Injection Devices

ONR/ARPA URI

Grant Number N00014-92-J-1895

Prepared by:

Paul H. Holloway
Department of Materials Science and Engineering
University of Florida
P.O. Box 116400
Gainesville, FL 32611
Ph: 904/392-6664; FAX: 904/392-4911
E-Mail: Internet-PHOLL@MSE.UFL.EDU

Participants:
University of Florida
Kevin Jones
Robert Park
Joeseph Simmons
Cammy Abernathy
Stephen Pearton
Dept. of Materials Science and Engineering
Timothy Anderson
Dept. of Chemical Engineering
Peter Zory
Dept. of Electrical Engineering
University of Colorado
Jacques Pankove
Dept. of Electrical Engineering
Columbia University
Gertrude Neumark
Dept. of Materials Science and Engineering
Oregon Graduate Institute of Science and Engineering
Reinhart Engelmann
Dept. of Electrical Engineering

(I) Molecular Beam Epitaxy Growth of II-VI and III-Nitrides (Robert Park)

(a) Widegap II-VI

We have continued this quarter to examine the mechanisms associated with lasing in widegap II-VI systems in collaboration with Dr. Robert Taylor of the University of Oxford.

We have performed time-resolved measurements of stimulated emission in $Zn_{1-x}Cd_xSe/ZnSe$ quantum well structures. We have measured the dependence of the emission energy and lifetime on excitation density both below and above the lasing threshold, and our results indicate that plasma effects may be important in specific structures.

The samples examined were a series of three $Zn_{0.8}Cd_{0.2}Se/ZnSe$ symmetric MQW structures with 10nm thick ZnSe barriers and 5, 10 and 13nm thick quantum wells, respectively. Substrates were removed by chemical etching so that the excitonic absorption spectrum could be measured. Luminescence was studied at 10K both in backscattering geometry, and also in cleaved cavities. Both short and long cavities, with respectively high and low optical losses, were studied so that the effects of lasing density threshold could be investigated. Luminescence was excited using subpicosecond pulses from a frequency-doubled Ti:sapphire laser, and detected using a streak camera with $\sim$20ps resolution.

At low excitation density we observed strong excitonic recombination displaying simple exponential decay kinetics. On increasing the density towards threshold, bilinear decay kinetics became apparent, with a very large radiative rate coefficient: for example, $R > 10^{11}$ cm^{-2} for the 13nm structure. The lifetime reduced dramatically as the threshold density was reached: in cleaved cavities the decay time was less than the instrumental resolution. Stimulated emission emerged at an energy below the free exciton absorption peak, and distinct cavity modes were observed. The magnitude of this shift (18meV at threshold) is consistent with decay mechanisms reported below in section (V), and is substantially smaller than the LO phonon energy (31 meV), ruling out the exciton-LO phonon mechanism. In the case of high efficiency cavities made from the 5nm and 10nm structures where low threshold densities were obtained, the stimulated emission energy did not change with increasing pump intensity, consistent with the results of Ding et al. [1]. However, in the case of high threshold cavities based on the 13nm structure, the emission line shifts quite clearly to low energy as the pump intensity is increased. This red shift is the hallmark of bandgap renormalization resulting from the formation of an electron-hole plasma. These observations are consistent with a gain mechanism involving localized excitons when lasing occurs at low carrier densities, but at high densities, it involves stimulated recombination from a correlated electron-hole plasma.

(b) Column III-Nitride

Work on column III-Nitrides was hindered this quarter due to the development of a leak in our MBE growth chamber. The leak was small and particularly difficult to locate but was finally pin-pointed to a weld on the source flange LN_2 cryo-shroud. Consequently, the large source flange had to be removed and the LN_2 cryo-shroud detached from the flange for repair. Fortunately, the weld could be repaired by the Engineering Machine Shop on campus which reduced our turn-around time.

The MBE growth chamber base pressure is now back to normal following an

extensive bakeout of the system and we have been able to duplicate some of our "standard" GaN runs.

Since the large source flange had to be removed from the chamber, we took this opportunity to clean out the inside of the growth chamber, removing flaking materials and debris. As a consequence of the cleaning process, we have noted a dramatic reduction in the intensity of a residual arsenic peak which appeared in our mass spectrometry analysis of the background gases. We believe that the MBE growth chamber is currently at its cleanest level since termination of our GaAs work.

(II) MOMBE Growth of III-N Alloys on (0001) ZnO Substrates (C. Abernathy and K. Jones)

Theoretically, the wurtzitic structures of $In_xGa_{1-x}N$ (x=0.17) and $In_xGa_{1-x}N$ (x=0.315) can be lattice matched to (0001) ZnO substrates (a=0.325nm, c=0.521nm). However, in order to grow high quality single crystal material, high quality ZnO substrates are required, having atomically smooth surfaces and low defect density ($<10^4/cm^2$).

ZnO substrates received from LMA were analyzed to determine the quality of the substrates. Their FWHM was determined, using a 5 crystal high resolution x-ray diffractometer, to be ~90 arc-secs (compare with ~15 arc-secs for epi-ready Si substrates). Also, tapping mode AFM measurements showed that the rms surface roughness of the ZnO substrates was ~1.5nm (compare with ~0.2nm for Si substrates). Attempts were made to reduce the surface roughness with a Syton polish, but there was no significant change in the rms roughness values.

In addition, annealing studies were carried out to determine the effect of nitrogen annealing on the surface of the ZnO substrate. Auger scans showed that there was no change in surface composition and stoichiometry for temperatures up to 500°C, which is the growth temperature for the nitride buffer layer.

(III) Ohmic Contact Formation (Paul Holloway)

(a) Degradation of Au/Pd/ZnTe/ZnSe Ohmic Contacts to p-ZnSe

Degradation studies of ZnTe/ZnSe contacts have continued with analytical data collected from the samples by Auger electron spectroscopy (AES), atomic force microscopy (AFM) and SEM. The sample structures consist of a top Au/Pd ohmic contacts on a ZnTe/ZnSe multiquantum well, then a p-ZnSe layer grown on p-GaAs (from 3M). The degradation was performed by mounting the samples on a copper heat sink connected to an APD cold finger, which also acted as the backside electrode. Power was supplied to the top Au/Pd contact, through a copper probe (tip radius of ~1 mm), to maintain a constant current density of ~30 A/cm^2 for times of 6 to 90 minutes. The temperature of the heat sink was controlled during degradation using the cold finger and was allowed to range from 300 K to 450 K. In later experiments, the copper probe was replaced with a gold probe, and a thermocouple was connected to the gold probe tip to measure the localized temperature rise at the point of contact, and this rise was found to be ~ 25 °C higher than that of the

heat sink.

AFM and SEM studies of the surface morphology indicate that degradation resulted in small rectangular raised features ($\sim$2 to 4 μm square) surrounding a $\sim$100 μm point of contact. These features appeared to be oriented with respect to the underlying ZnTe, suggesting the formation of a textured or epitaxed phase. Preliminary attempts to identify the structure and composition of this phase were inconclusive, but TEM analysis is underway to precisely identify the nature of these features.

These raised features are of particular interest since removing the overlying Au/Pd contacts by wet chemical etching and by ion beam sputtering revealed elongated cracks lying along the edges of the raised features. These cracks extended through the ZnSe layer and into the GaAs substrate. In addition, preliminary measurements indicate that the cracks are parallel to the <100>directions, similar to the formation of dark line defects which quench light emission in ZnSe based diodes and laser diodes.

Auger depth profiles indicate there is a substantial loss of Zn from the underlying ZnSe following degradation. These data also suggest that there is a high reactivity between Pd from Au/Pd contacts and the underlying Zn, Se and possibly Te. Further experiments are also underway to determine the exact reactions which occur. Apparently, high current and/or local heating caused more rapid degradation of these contacts versus simply isothermal heat treatments of Au/ZnTe contacts.

(b) Au/ZnTe Electrical Contacts

Studies of Au electrical contacts on p-ZnTe have continued. Previously the 1000 Å Au films were analyzed by current-voltage (I-V) measurements to determine stability upon post deposition annealing. It was found that at 350°C for 15 minutes the resistance increased by a factor of 25. Auger depth profiles on the sample annealed at 350°C showed diffusion of Au throughout the ZnTe capping layer. Secondary ion mass spectrometry (SIMS) results on samples annealed at 250°C and 350°C for 90 minutes showed that the Au diffused much further into the ZnTe layer with the higher temperature. Scanning electron microscopy (SEM) on the 350°C sample showed regions of the Au layer bubbling up and separating from the ZnTe. These results are currently being prepared for publication.

(c) GaN Contacts

Au and Au/Ni contacts to p-GaN were deposited by sputtering and electron beam evaporation. All contacts showed rectifying behavior as deposited. Heat treatments of 200°, 400°, and 600°C were performed for times of 5, 15, and 30 minutes. The estimated barrier height of the Schottky contacts was lowered by heat treatment at the two highest temperatures for both contact schemes. An Auger depth profile of the Au/Ni sample annealed at 600°C for 30 minutes showed diffusion of the Ni interlayer through the Au layer and to the surface of the sample. SEM showed coalescence into islands of the Au layer at 600°C for 15 minutes without the Ni layer, while coalescence was not observed upon inclusion of the Ni layer.

(IV) Microstructural Analysis of II-VI and III-V Materials (Kevin Jones)

a) Electrical Degradation Study of II-VI LED Structures

Microstructural changes in degraded II-VI LED structures have been studied using TEM and EL microscopy. LED's were degraded by applying a pulsed current to a device with a large area of electrical contact for easier characterization. Au was deposited using an e-beam evaporator over the entire surface of the sample. The sample was subsequently cut into small pieces(2 mm x 2 mm) for degradation and TEM investigation. The intensity and spectrum of the light emitted from the edge during degradation was measured by a spectrometer so that the degree of degradation could be controlled. For the [100] dark line investigation, a sample was degraded down to 20 % of the initial output intensity. The structure of the degraded sample consisted of a ZnSe-ZnTe graded ohmic contact / p-type ZnMgSSe / p-type ZnSSe / ZnCdSe quantum well / n-type ZnSSe / n-type ZnMgSSe / on the GaAs substrate.

TEM samples were prepared after degradation. For plan- view TEM samples, the sample was ion milled from the backside (substrate) first until a hole was obtained and then gradually ion-milled from the top surface in order to reach the quantum well region. The samples were examined with TEM after every 10 minutes of ion-milling in order to observe degradation induced defects throughout each of the layers.

Dislocations of the type [110] developed mostly at the interface between the upper cladding layer(ZnMgSSe) and barrier layer (ZnSSe) during operation. These dislocations appeared to be connected to preexisting misfit dislocations located at the graded contact and ZnMgSSe interface. Some of these dislocations appear to originate from preexisting stacking faults.

Dark line defects(DLD) of [100] type were observed for the first time in these studies by TEM. These line defects appeared to be generated around the ZnCdSe quantum well and were not dislocation networks, contrary to observations in III-V device structures. The DLDs appear to be comprised of smaller defects connected along the [100] direction (Figs. IV.1 and 2). These smaller defects appear to be similar to point defects clusters that occur in areas where the crystal lattice has been damaged.

Other unknown degradation induced defects (labeled U in Fig. IV.1) were also observed, especially near the active region. In order to understand the evolution of DLD's and other defects during operation, TEM investigations of less degraded sample are in progress.

b) Characterization of nitride-based compound semiconductors

The influence of epilayer thickness on the film quality and the film/substrate interface was studied by cross-sectional transmission electron microscopy (XTEM) in the GaN/Al_2O_3 system.

Samples with different epilayer thicknesses were grown under identical conditions using MOCVD on (0001) Al_2O_3. Prior to the growth of the epitaxial film, 50 nm thick low temperature GaN buffer layer was grown at 600°C. The epilayer was grown at 850°C.

XTEM bright-field images were obtained using two-beam diffraction condition with diffraction vector $g=(2\,\underline{1}\,\underline{1}\,0)$, of the alpha-GaN films grown on (0001) Al_2O_3. The film quality seemed to have improved with an increased thickness of the epilayer. The

Fig. IV.1. Low magnification TEM micrograph showing [100] dark line defects (DLD) and other unknown defects (labeled U).

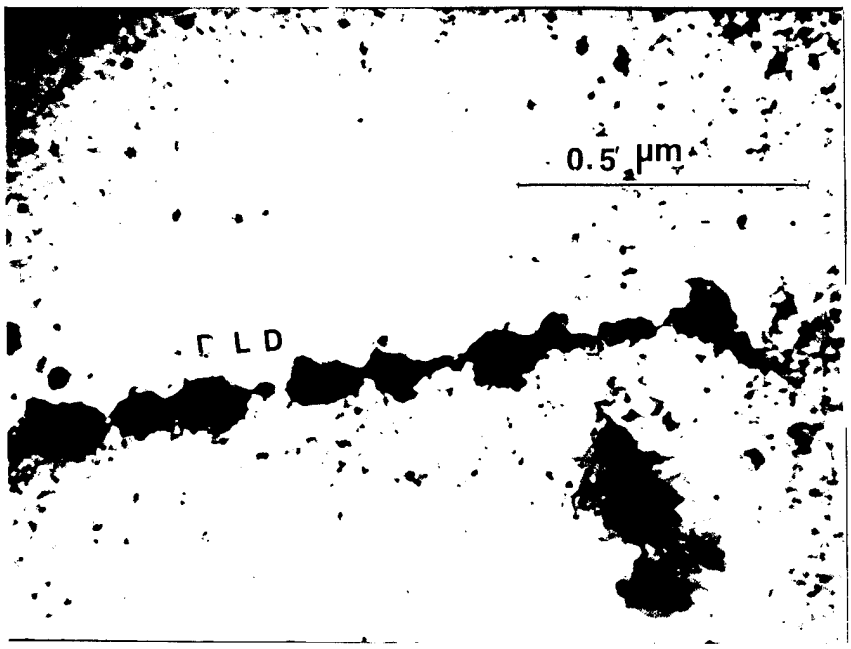

Fig. IV.2. TEM micrograph of a closer view of a [100] dark line defect showing that it is comprised of other defects.

film/substrate interface was smooth and abrupt with no indication of interfacial phases. However, due to the large in-plane lattice mismatch as well as the buffer layer/substrate thermal-expansion mismatch, the film contained a high concentration of threading dislocations. We will next attempt to identify the defects present in the film and to study how these defects change with growth conditions.

(V) Optical and Electrical Characterization of ZnSe (J.H. Simmons)

During the past quarter, we have conducted measurements at 10K of photoexcited carrier lifetimes in $Cd_xZn_{1-x}Se/ZnSe$ ($x=0.2$) quantum wells grown on GaAs or on ZnSe substrates. The photoluminescence data show both exciton and biexciton transitions with lifetimes of 266 and 108 ps, respectively. These data are consistent with the time resolved PL measurements reported in (Ia) above. We are now measuring the effects of barrier width on these lifetimes.

(VI) MOCVD Growth of GaN Thin Films (Tim Anderson)

We previously reported success in MOCVD growth of α-GaN films on Al_2O_3 and 6H-SiC substrates. The growth conditions were optimized on these unpatterned substrates in the 650 to 850°C temperature range. A study of the effects of known catalysts (e.g., W and Mo) on the growth of GaN on sapphire substrate has been started. These catalysts are known to enhance the thermal decomposition of NH_3. Patterned Al_2O_3 substrates with W and Mo lines with different widths and separations were provided by Dr. Arnold Howard of Sandia National Lab.

The growth of GaN on patterned substrates at 76 Torr and 650, 750 and 850°C. The quality of GaN films were characterized by X-ray diffraction (XRD) and scanning electron microscopy (SEM). The X-Ray diffraction peak corresponding to (0002) reflection of wurtzite GaN were after each of the three growth temperatures. The crystallinity improves with increasing substrate temperature. We attribute this improvement to enhanced decomposition of NH_3 as a result of increased catalytic activities of W and Mo at elevated temperatures. The SEM images from patterned substrates also indicate similar hexagonal GaN surface feature in the trench, similar to unpatterned Al_2O_3 substrates. However, growth occurred predominantly in the trenches rather than on the W and Mo metal masks. Except for some decoloration, the W line maintained its surface integrity even up to 900°C in the GaN growth environment. On the other hand, Mo metal lines suffered surface degradation. Further characterization of these samples is in progress.

Light emission from GaN films is typically associated with an undesirable strong yellow peak at 2.15 eV and a weaker edge luminescence at 3.4 eV. Ms. Li Wang (Dr. Joe Simmons's group) has used low temperature photoluminescence (PL) measurements to support improvements in the optical quality of our GaN films grown on unpatterned Al_2O_3 substrates. As shown in Fig. VI.1, this yellow peak is very low (reduced by an order of magnitude) in GaN film grown at 750°C.

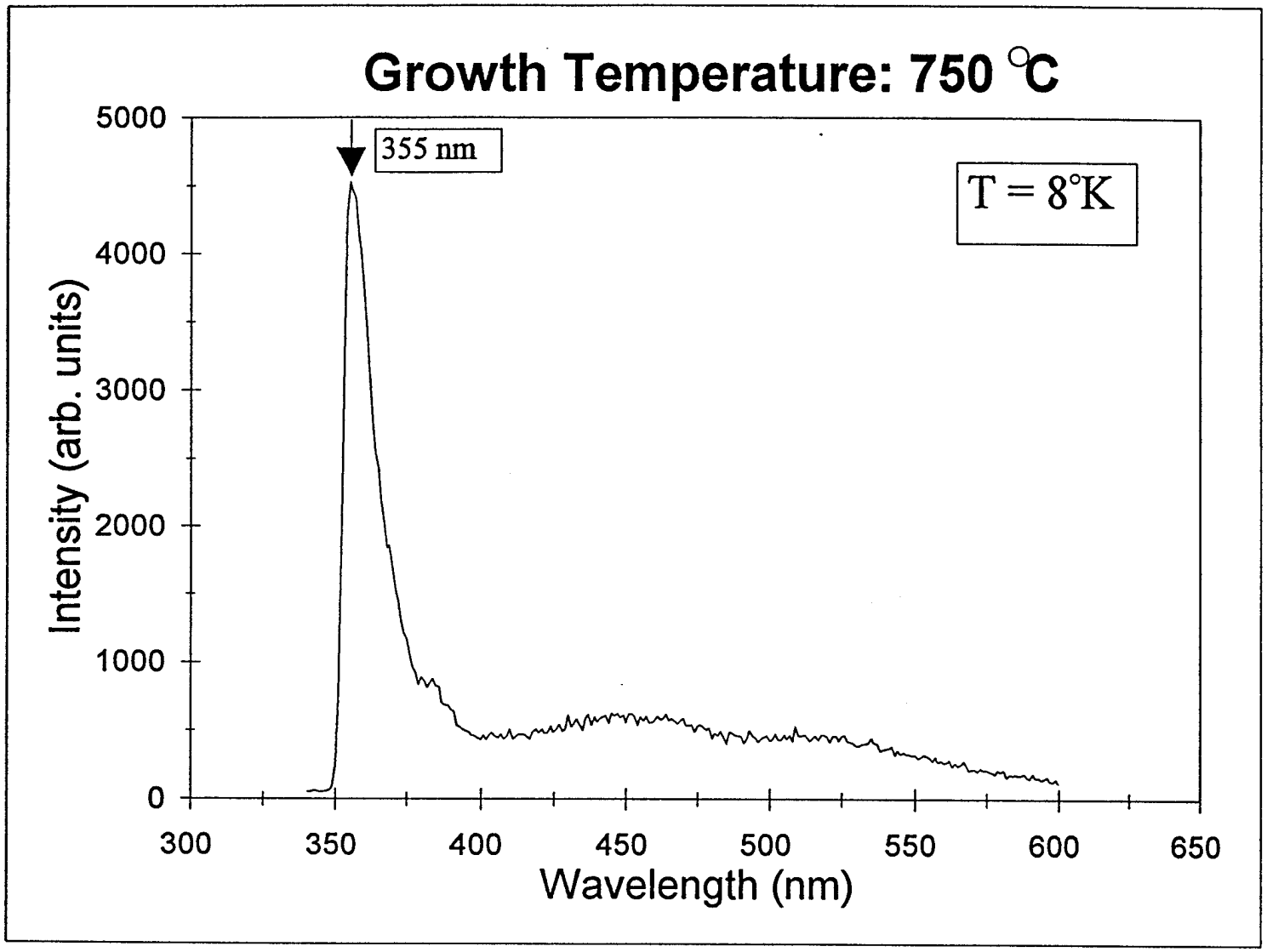
Growth Temperature: 750 °C
355 nm
T = 8°K
Intensity (arb. units)
5000
4000
3000
2000
1000
0
300
350
400
450
500
550
600
650
Wavelength (nm)

Fig. VI.1.

(VII) Development of Diode Lasers (Peter Zory)

(a) Diode Pumping

Using a novel, pulsed electro-chemical pumping technique in conjunction with modeling, we have demonstrated that one can determine the non-radiative decay rate in the quantum well layer(s) of diode laser material. Since the technique uses unprocessed laser material and is non-destructive, one can fabricate diode lasers from the material studied and determine if the measured decay rate correlates with laser reliability. This new technique is being studied for evaluation of the standard surface-emitting LED devices that used previously in our CdZnSe laser material degradation studies.

(b) Photopumping

Work is continuing in the evaluation of GaN-based materials using the 337 nm nitrogen laser.

(VIII) Theoretical Calculations of Dopants of ZnSe (Gertrude Neumark)

As mentioned in the preceding progress report, the ionic contribution to the screenings should be considered for a proper analysis of the temperature dependence of conductivity. This contribution consists of two parts: 1) Screening resulting from ionic motion at high temperatures, with such motion stopping at a temperature T_m, where this screening stops [G.F. Neumark, Phys. Rev. **B5**, 402 (1972)]. 2) A preferential capture of carriers at certain dopant ions, determined by potential fluctuations, which provide deeper "wells"at these "favored" impurities [discussed for instance in G.F. Neumark, J. Appl. Phys., **48**, 3618 (1977)].

We have applied an efficient fitting procedure to analyze data of carrier concentration vs. temperature with consideration of linear screening effects. In this analysis, we have neglected the T_m contribution. Since ZnSe:N layers are generally grown at low temperatures ($\sim$500 K), we assume that N is not mobile at growth temperatures. With use of linear screening due to free carriers and above-mentioned preferential ion neutralization, we obtained a good fit of theoretically obtained values to Hall data of Han et al. [J. Cryst. Growth, **138**, 464, (1994)] (see Fig. VIII.1). We note that our results for impurity concentrations are about 20% lower than Han's values. Our value for the activation energy at room temperature is about 82 meV. We thus obtain good fits to <u>both</u> optical and electrical data by use of screening. Moreover, we expect even larger differences in electrical parameters with inclusion of screening than the above for more heavily compensated material.

As mentioned, the above analysis assumes linear screening. Also, we have neglected broadening of the energy distribution of the impurity levels. Neither of these factors is likely to lead to serious errors for sample we have considered, where the compensation is relatively low. However, corrections may be required for analyses of heavily compensated samples, to which we would like to extend our analyses.

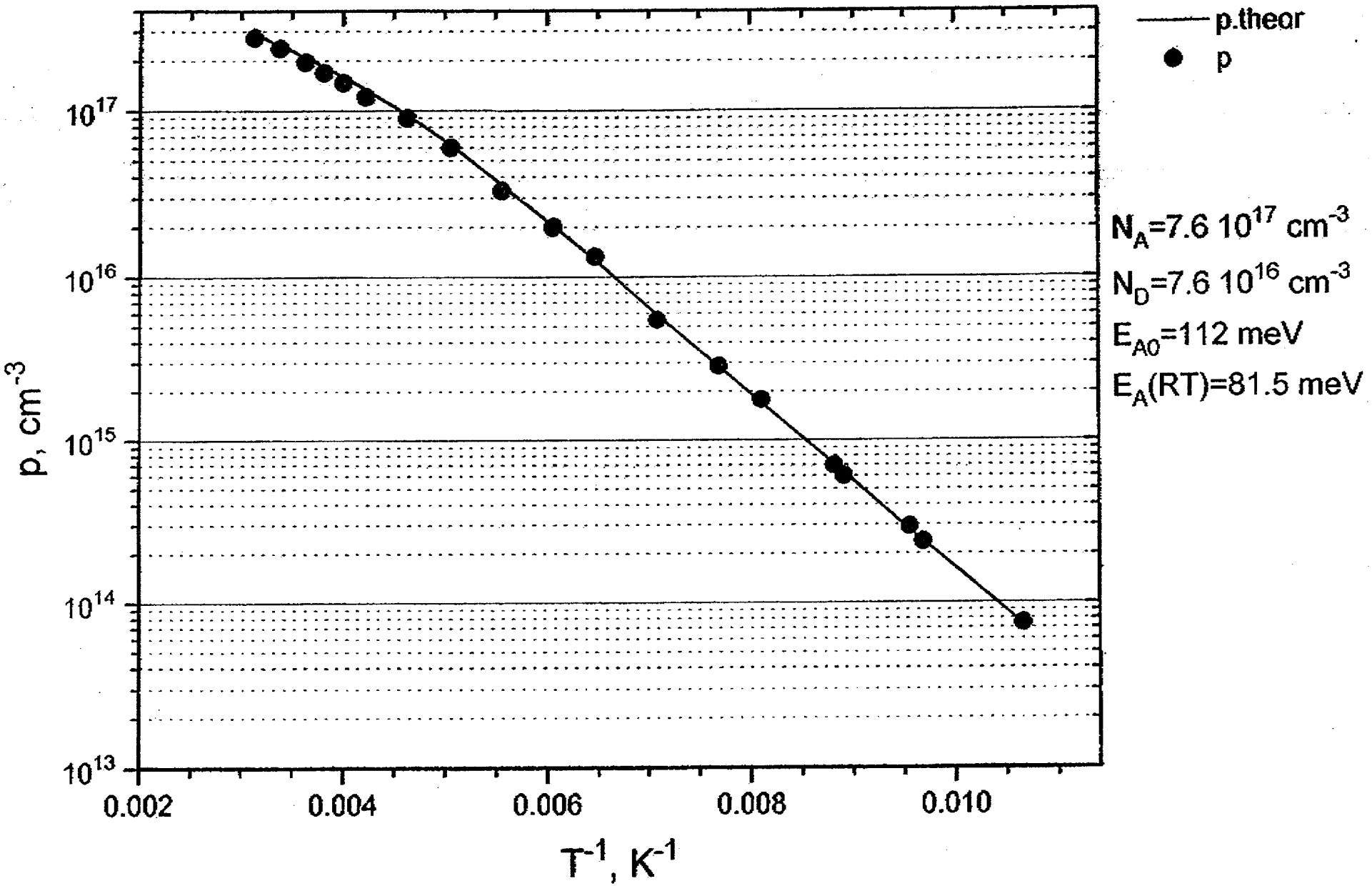

Fig. VIII.1. Hole concentration calculated with consideration of screening effects, filed to data of Han et.al.

(IX) MOCVD Growth of GaN (Jacques Pankove)

Our objective is to grow p-n junctions in GaN that will be the basis for short wavelength emitters and lasers. Our material growth efforts this quarter have centered on optimization of the GaN buffer layer. We have increased the maximum mobility to 255 $cm^2/V\text{-}s$ and are still trying to reduce the as-grown electron concentration. Our goal is to reach an as-grown electron concentration of $\sim 1 \times 10^{17} cm^{-3}$ or lower while maintaining high mobility. We would then begin doping studies and growth of p-n junctions.

We have continued our examination of forbidden-gap states in GaN, focusing on the 2.15eV yellow peak that commonly appears in photoluminescence spectra of undoped GaN.[1] Luminescence measurements utilizing a finely focused laser spot or electron beam revealed structure in this peak (Fig. IX.1) observable at both 6K and room temperature. The observation of a number of equally spaced peaks is strongly suggestive of phonon replicas. Strong phonon coupling is expected for radiative recombination involving deep states, increasing with the depth of the level.[2] The phonon energy is $\approx$ 100meV which is close to the LO phonon value of 92meV. We plan to use the procedure of Monemar and Samuelson[3] to deconvolve the electronic (no-phonon) peak position and lineshape from the observed spectrum.

It has been suggested that the 2.15eV luminescence peak is due to the transition from the conduction band (or a shallow donor) to a defect level somewhat above the valence band edge[4]. In order to explore this idea, we tried to quench the yellow luminescence by pumping electrons from the valence band to the defect state via infra-red illumination. As the electron occupation of the defeat states increases, the luminescence intensity of the yellow peak should decrease. For this experiment, we used a He-Cd laser at 325nm for intrinsic excitation across the gap and 980nm diode laser for the IR pumping. We found that quenching is indeed observed and we measured a change in yellow intensity of up to eight percent. Figure IX.2 shows a portion of the room temperature photoluminescence spectrum of an undoped GaN sample both with and without the IR pumping. In addition, we also measured the photoluminescence quenching (PLQ), defined as

$$\Delta I = \frac{I_{yellow} - I_{yellow,\,IR}}{I_{yellow}}$$

as a function of the intensity of the UV excitation. Figure IX.3 shows that ΔI decreased rapidly with an increase in UV excitation intensity. We hope to explain this observation through further work. In the future we plan to measure the IR wavelength dependence of the PLQ to determine the energy cutoff of the quenching effect and hence determine the depth of the level above the valence band.

[1] J. Ding, et. al., Phys. Rev. Lett., **69**, 1707 (1992).

[2] J.I. Pankove, Optical Processes In Semiconductors (Prentice-Hall, New York, 1971), p.139.

[3] B. Monemar, L. Samuelson, Physical Review B, **18**, p.809 (1978).

[4] M.W. Leksono, C.H. Qiu, W.Melton and J.I. Pankove, Mat. Res. Soc. Symp. Proc., **339**, p.559 (1994).

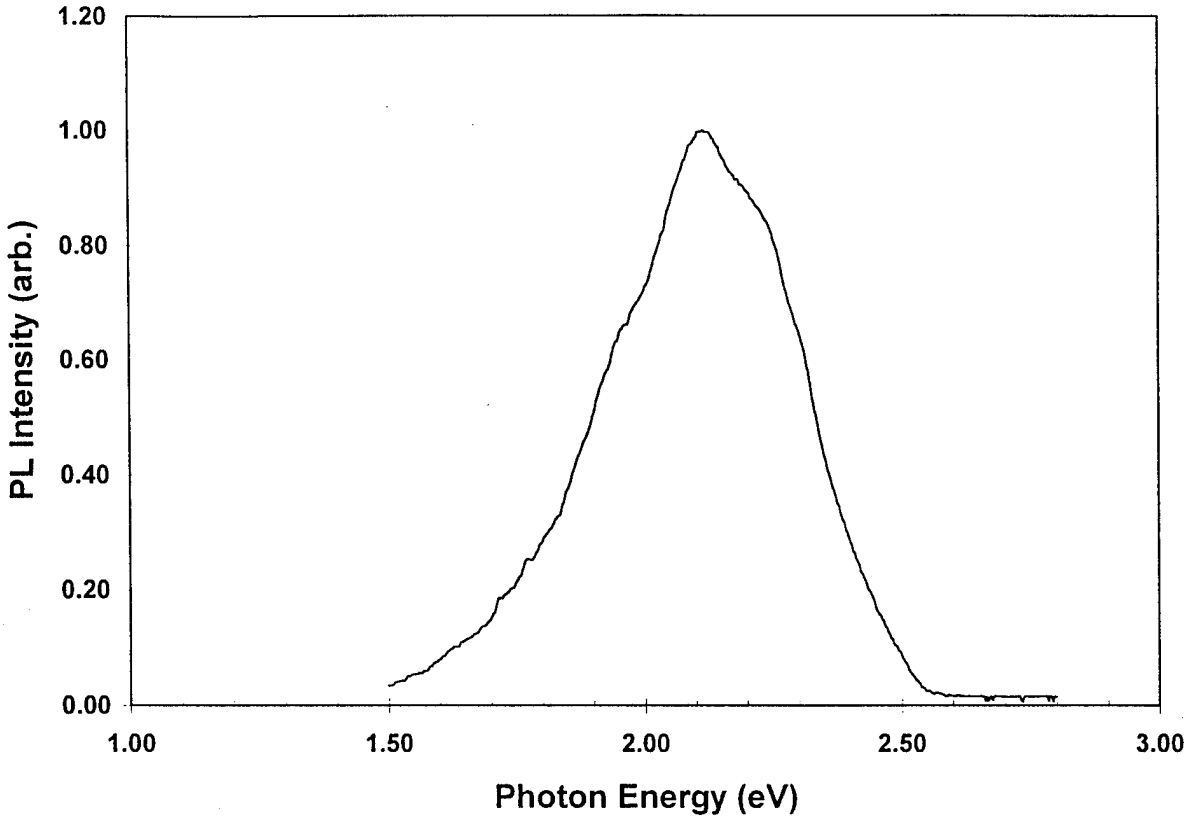

Fig. IX.1. Photoluminescence spectrum of undoped GaN at 6K showing structure in 2.15eV peak.

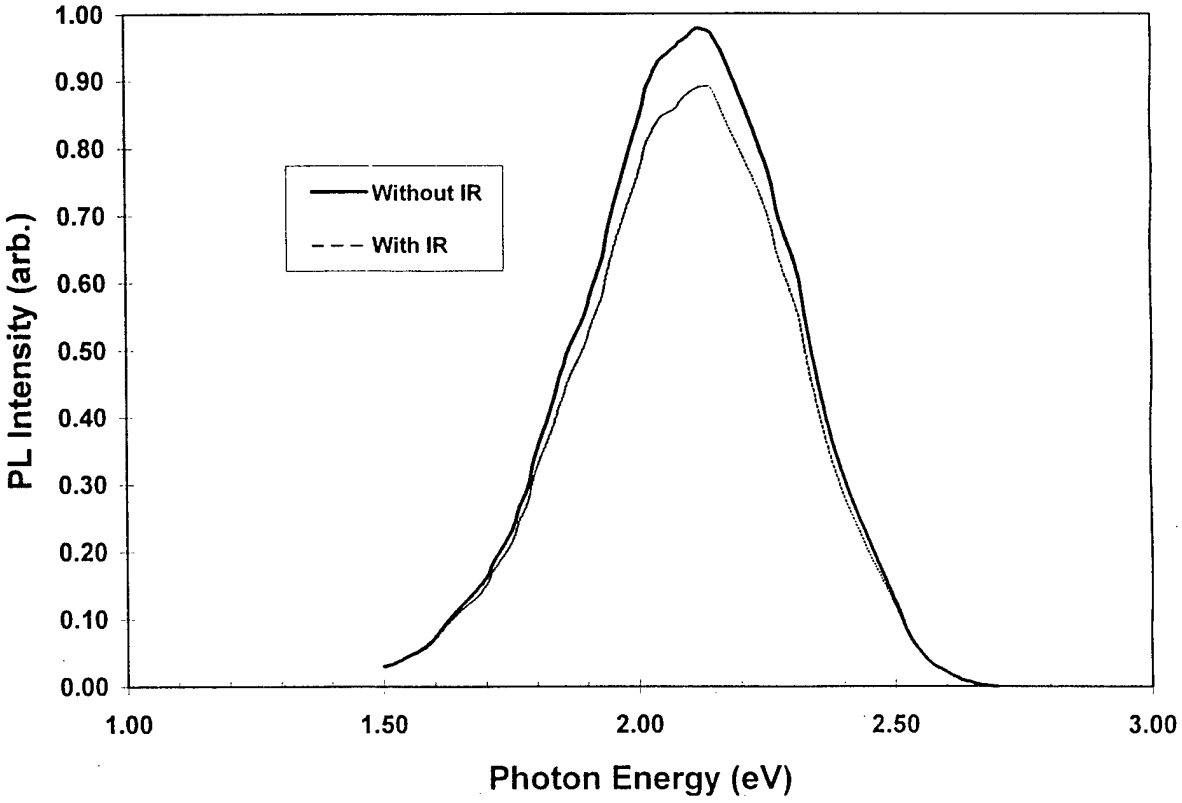

Fig. IX.2. Room temperature photoluminescence spectra of undoped GaN both with and without 980nm IR illumination.

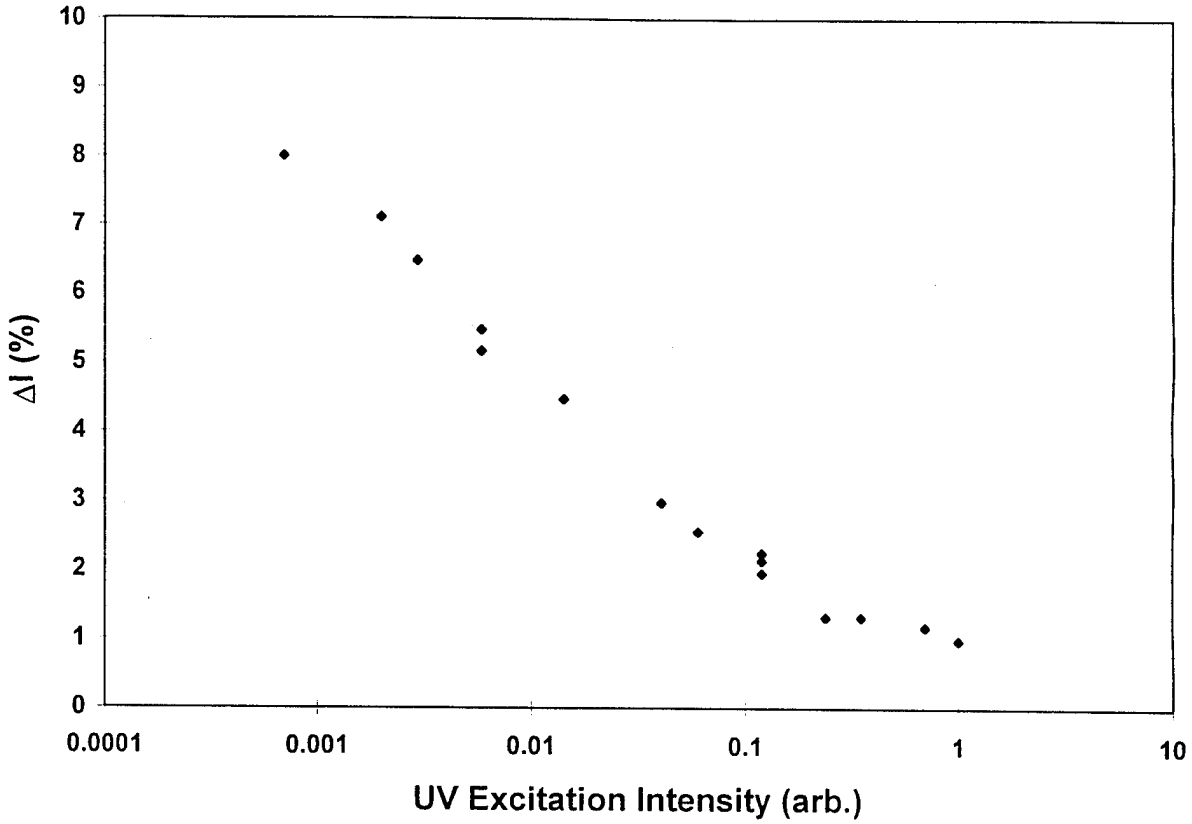

Fig. IX.3. IR Photoluminescence quenching as a function of intrinsic UV excitation intensity.

(X) Gain Modeling in II-VI Strained-Layer QW Structures (Reinhart Engelmann)

A new two-dimensional laser diode simulation software has been evaluated. A simple band-gap calculation program has also been modified and will be used to calculate the band structure of zinc-blende II-VI and III-V nitride materials.

a) Two-Dimensional Device Simulation

A new two dimensional device simulation software package from SILVAC International has been installed in EEAP department computer system. Contrary to the MEDICI software that we used for the work covered in our previous report, the new software has the capability of directly modeling optoelectronic devices. MEDICI does not contain a Helmholtz-equation solver. Therefore we had been using MODIEG (courtesy of Gary Evans, Southern Methodist University) for optical confinement calculations. The SILVACO package has the complete capability for full heterojunction device and DH laser simulation. The user can also specify the gain model allowing the simulation of QW lasers.

The laser simulator performs coupled electrical and optical simulation of semiconductor lasers by solving the Helmholtz equation in conjunction with modeling of heterojunction drift-diffusion equations. Two types of simulations are available. The first one is a fast model for single frequency calculation. (User specifies the laser frequency and losses.) The second one takes more time which strongly depends on the number of longitudinal modes involved in the calculation (by specifying the cavity length). So far the software supports the III-V materials such as the GaAs/AlGaAs and InP/InGaAsP systems. New material systems can be incorporated by defining the relevant material parameters, e.g., band gap and effective mass. The 2-D simulator is particularly useful in analyzing the lateral current distribution in a stripe-geometry, gain-guided device, as well as in devices with more advanced design, such as buried-heterostructure lasers. Figs. X.1, 2 and 3 show some simulation examples for an InP/InGaAsP device to demonstrate the SILVAC capabilities. Conversion to II-VI and GaN-based structures is in progress.

b) Band Structure Calculations

A more detailed knowledge of the band structure of the newer II-VI and III-V nitride materials is desirable for proper QW gain modeling, particularly with carrier spill-out effects. For this reason, an existing band-structure calculation program based on the semiempirical extended Huckel theory[1] has been modified, allowing band simulations of several materials of interest such as zinc-blende CdSe, GaN, ZnS and CaS. The work is conducted in cooperation with Dr. Christopher Barbero of EEAP at OGI.

c) Future Plan

We intend to apply the 2-D simulator to advanced blue-green II-VI laser structures in order to investigate the influence of lateral current and gain confinement on the laser performance. Additionally, we plan to analyze the band gap structure for cubic GaN and InN for modeling a InGaN laser.

[1] Satya N. Sahu,"Defect Studies in Semiconductors", Ph.D dissertation, SUNY at Albany, 1982.

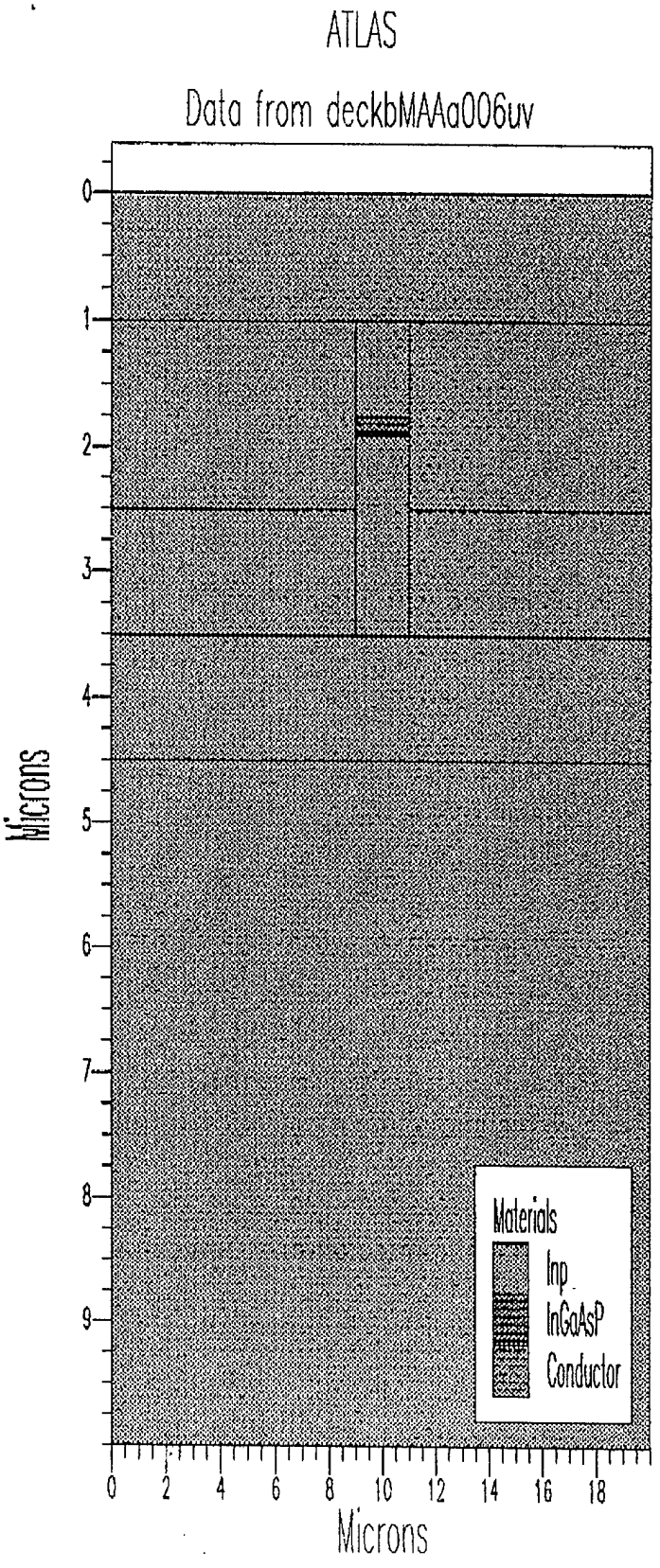
ATLAS
Data from deckbMAAa006uv
Microns
Microns
Materials
Inp
InGaAsP
Conductor

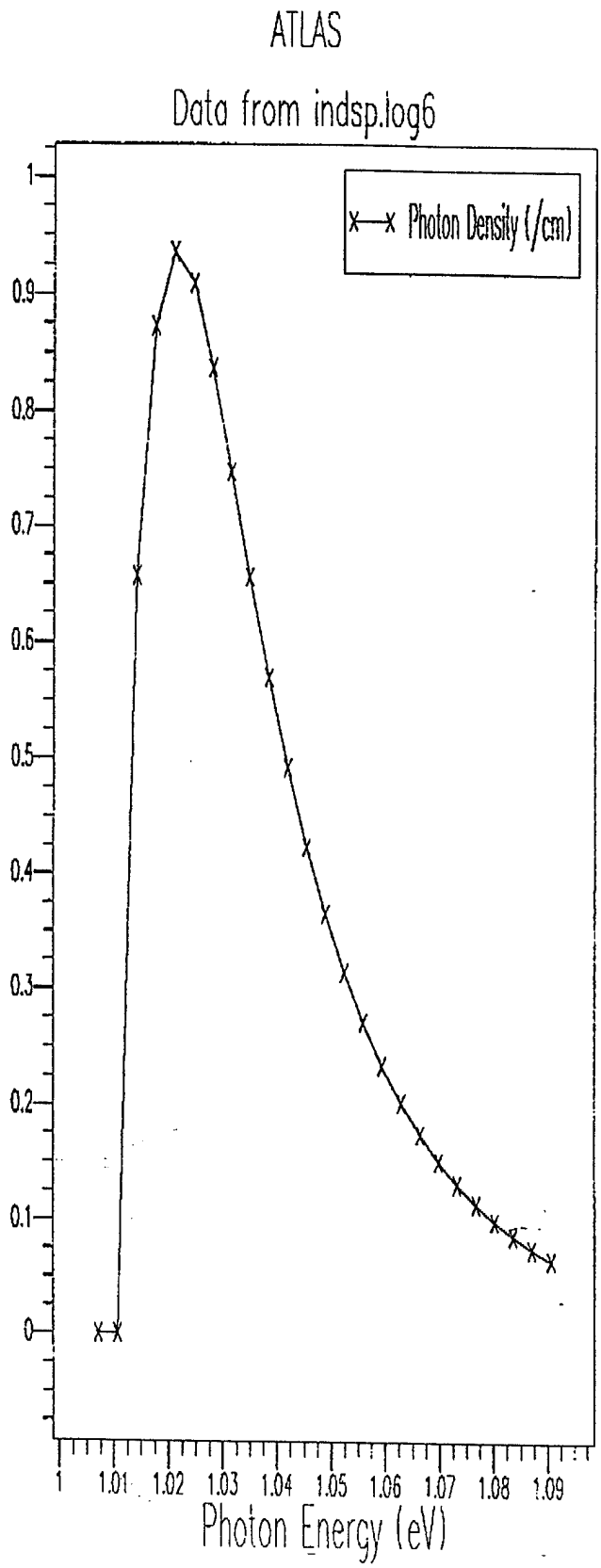
ATLAS
Data from indsp.log6
Photon Density (/cm)
Photon Energy (eV)

Fig. X.1.

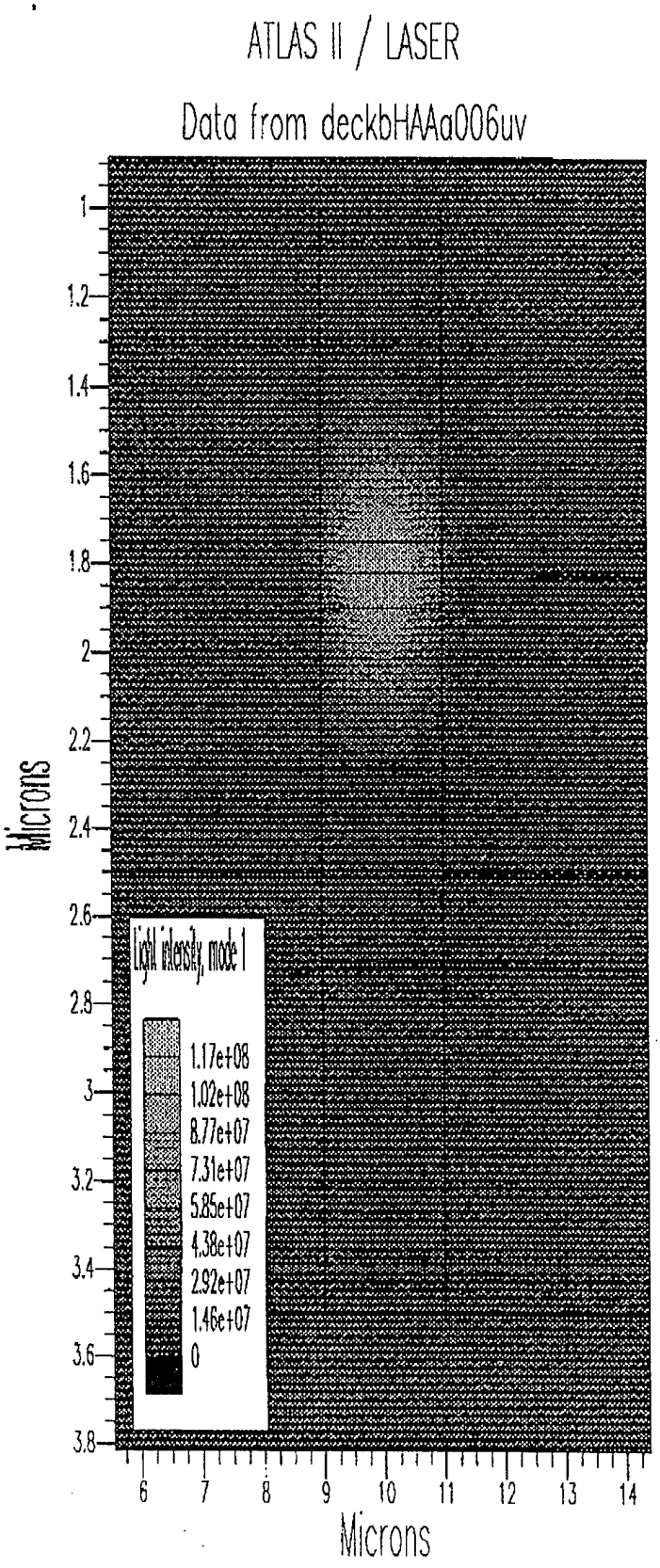
ATLAS II / LASER
Data from deckbHAAa006uv
Microns
Microns
Light intensity, mode 1
1.17e+08
1.02e+08
8.77e+07
7.31e+07
5.85e+07
4.38e+07
2.92e+07
1.46e+07
0

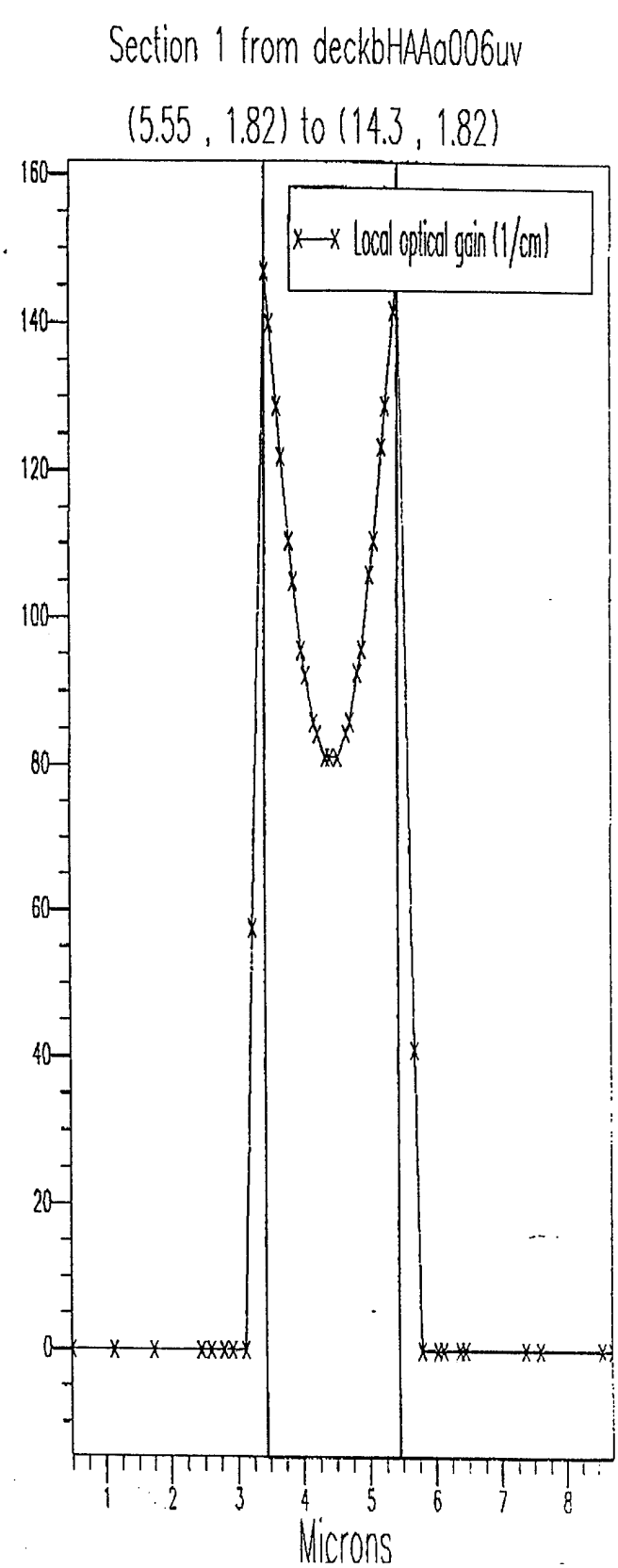
Section 1 from deckbHAAa006uv
(5.55 , 1.82) to (14.3 , 1.82)
Local optical gain (1/cm)
Microns

Fig. X.2.

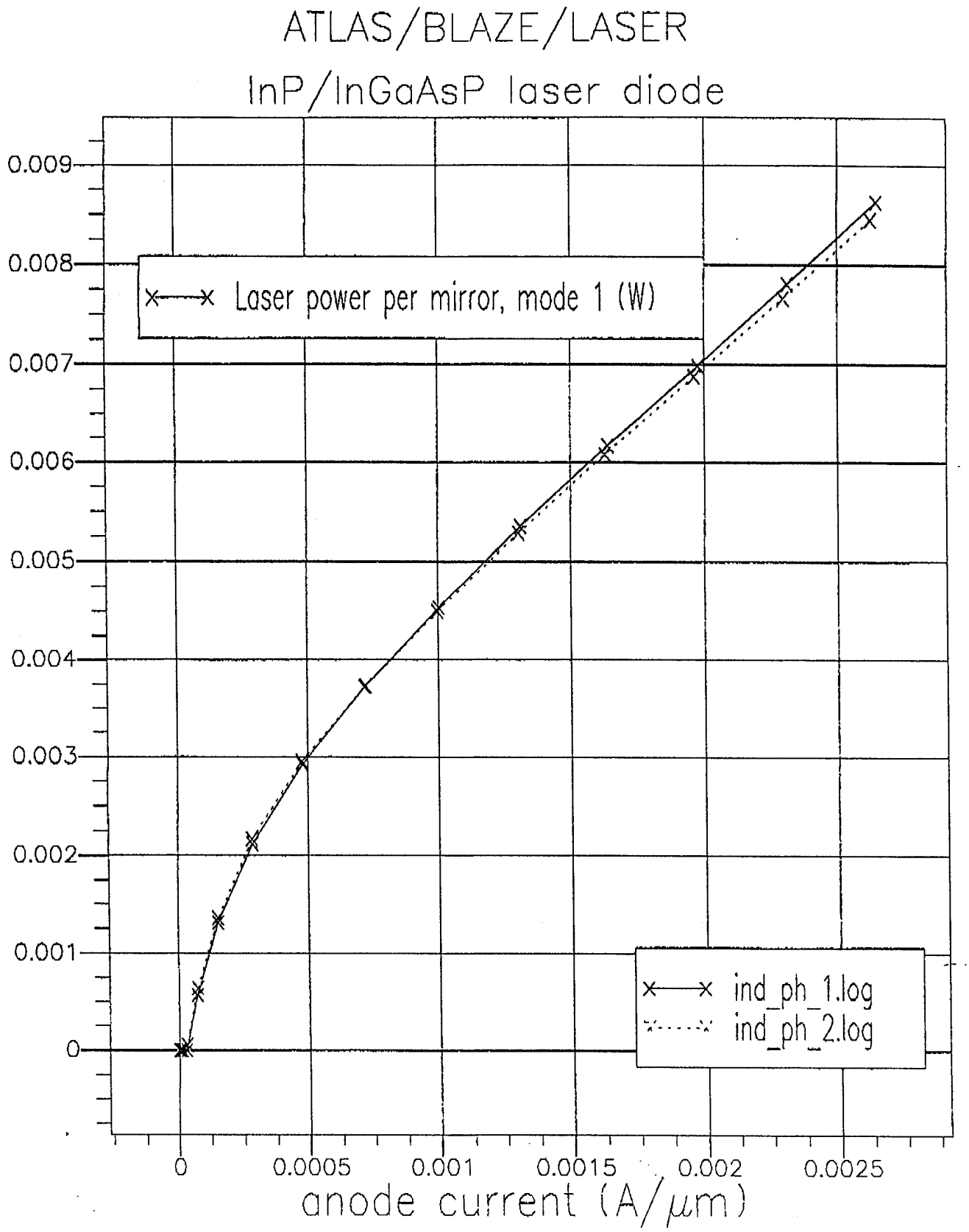
ATLAS/BLAZE/LASER
InP/InGaAsP laser diode
Laser power per mirror, mode 1 (W)
ind_ph_1.log
ind_ph_2.log
0.009
0.008
0.007
0.006
0.005
0.004
0.003
0.002
0.001
0
0
0.0005
0.001
0.0015
0.002
0.0025
anode current (A/μm)

Fig. X.3.

Honors

- P.S. Zory received the Distinguished Lecturer Award for 1995/1996 from the IEEE Lasers and Electro-Optics Society - lecture subject is "Blue-Green Quantum Well Lasers."

Presentations this quarter

- "Ohmic Contacts to n-GaN," S. Miller, P. Holloway and J. Pankove, MRS Spring Meeting, San Francisco, CA, April 17-21, 1995.

- "Blue-Green Semiconductor Lasers" at the 25th Winter Colloquium on Quantum Electronics, P.S. Zory - Snobird, Utah - 4 Jan 1995.

- "Blue-Green Diode Lasers: Technology Status" at the Spring Meeting of the Materials Research Society, P.S. Zory - San Francisco, CA - 17 April 1995.

- "Blue-Green Diode Lasers for Optical Memory Applications" - Press Conference at Materials Research Society Meeting, P.S. Zory - San Francisco, CA - 17 April 1995.

- " Quantum Well Lasers" at the IEEE Princeton/Sarnoff Symposium, P. Zory - Princeton, NJ - 28 April 1995.

- "Let light emitting diodes (LEDs) shine!" Seminar, Optical Society of America, - R. Engelmann.
  1) Columbia Section, Portland, OR, 27 January 1995.
  2) Puget Sound Chapter, Seattle, WA, 16 May 1995.

- "Photonics at the Oregon Graduate Institute of Science & Technology," Seminar, R. Engelmann, Electrical Engineering Department, University of Washington, 17 May 1995.

- "Comparison of the Quality of MOVPE GaN Films on Various Substrates", Akhter U. Ahmed, Ziad Osman, and Timothy J. Anderson, Seventh Biennial Workshop on Organometallic Vapor Phase Epitaxy, Fort Meyer, Florida, April, 1995.

Short Course:

- "Visible Semiconductor Lasers" at the Conference on Electro-Optics and Lasers, P.S. Zory - Baltimore, MD - 25 May 95.

Conference Activity:

R.M. Park, Chairman and co-organizer of symposium on "Visible Light Emitting Materials and Devices" at the Spring '95 MRS Meeting in San Francisco, April 17-21, 1995.

Post Doctoral Associates, Graduate Research Assistants, and Undergraduate Research Assistants:

Post Doctoral Associates:

Akhter Ahmed with Dr. Anderson
Ziad Osman with Dr. Anderson
Viswanath Krishnamoorthy with Dr. Jones
Moeljanto Leksono with Dr. Pankove
Chang-hua Qiu with Dr. Pankove

Graduate Research Assistants:

Bruce Liu with Dr. Park
Minhyon Jeon with Dr. Park
George Kim with Dr. Park
Jeff Hsu with Dr. Zory
Jason O. with Dr. Zory
Igor Kuskovskiy with Dr. Neumark
Li Wang with Dr. Simmons
Y. Cai with Dr. Engelmann
Charles Hoggatt with Dr. Pankove
William A. Melton with Dr. Pankove
John Fijol with Dr. Holloway
T.J. Kim with Dr. Holloway
Jeff Trexler with Dr. Holloway
Steve Miller with Dr. Holloway
Eric Bretschneider with Dr. Anderson
Joe Cho with Dr. Anderson
Todd Dan with Dr. Anderson
J. Kim with Dr. Jones
S. Bharatan with Dr. Jones
S. Bhendi with Dr. Jones

Undergraduate Research Assistants:

Julie Sauer with Dr. Simmons
Bob Covington with Dr. Anderson
Michael Mui with Dr. Anderson
Brendon Cornwell with Dr. Anderson

f:qprdoc.072